Core-to-Rydberg band shift and broadening of hydrogen bonded ammonia clusters studied with nitrogen K-edge excitation spectroscopy

Takeshi Yamanaka, Kiyohiko Tabayashi, Osamu Takahashi, Kenichiro Tanaka, Hirofumi Namatame et al.

Citation: J. Chem. Phys. **136**, 014308 (2012); doi: 10.1063/1.3673778
View online: http://dx.doi.org/10.1063/1.3673778
View Table of Contents: http://jcp.aip.org/resource/1/JCPSA6/v136/i1
Published by the AIP Publishing LLC.

Core-to-Rydberg band shift and broadening of hydrogen bonded ammonia clusters studied with nitrogen *K*-edge excitation spectroscopy

Takeshi Yamanaka,[1] Kiyohiko Tabayashi,[1,2,a)] Osamu Takahashi,[1] Kenichiro Tanaka,[1,3] Hirofumi Namatame,[1,2] and Masaki Taniguchi[1,2]
[1]*Graduate School of Science, Hiroshima University, 1-3-1 Kagamiyama, Higashi-Hiroshima 739-8526, Japan*
[2]*Hiroshima Synchrotron Radiation Center (HSRC), Hiroshima University, 2-313 Kagamiyama, Higashi-Hiroshima 739-0046, Japan*
[3]*XFEL Division, Japan Synchrotron Radiation Research Institute, 1-1-1 Kouto, Hyogo 679-5198, Japan*

(Received 9 October 2011; accepted 10 December 2011; published online 5 January 2012)

Nitrogen 1*s* (N l*s*) core-to-Rydberg excitation spectra of hydrogen-bonded clusters of ammonia (AM) have been studied in the small cluster regime of beam conditions with time-of-flight (TOF) fragment-mass spectroscopy. By monitoring partial-ion-yield spectra of cluster-origin products, "cluster" specific excitation spectra could be recorded. Comparison of the "cluster" band with "monomer" band revealed that the first resonance bands of clusters corresponding to N $1s \rightarrow 3sa_1/3pe$ of AM monomer are considerably broadened. The changes of the experimental core-to-Rydberg transitions ΔFWHM (N $1s \rightarrow 3sa_1/3pe$) = $\sim$0.20/$\sim$0.50 eV compare well with the x ray absorption spectra of the clusters generated by using density functional theory (DFT) calculation. The broadening of the core-to-Rydberg bands in small clusters is interpreted as being primarily due to the splitting of non-equivalent core-hole N 1*s* states caused by both electrostatic core-hole and hydrogen-bonding ($H_3N\cdots H–NH_2$) interactions upon dimerization. Under *Cs* dimer configuration, core-electron binding energy of H−N (H-donor) is significantly decreased by the intermolecular core-hole interaction and causes notable redshifts of core-excitation energies, whereas that of lone-pair nitrogen (H-acceptor) is slightly increased and results in appreciable blueshifts in the core-excitation bands. The result of the hydrogen-bonding interaction strongly appears in the $n-\sigma^*$ orbital correlation, destabilizing H−N donor Rydberg states in the direction opposite to the core-hole interaction, when excited N atom with H−N donor configuration strongly possesses the Rydberg component of anti-bonding σ^* (N−H) character. Contributions of other cyclic H-bonded clusters $(AM)_n$ with $n \geq 3$ to the spectral changes of the N $1s \rightarrow 3sa_1/3pe$ bands are also examined. © *2012 American Institute of Physics*. [doi:10.1063/1.3673778]

I. INTRODUCTION

Since inner-shell electron excitation deals with the transition of an electron localized closely to a nucleus (core-atom) into unoccupied electronic levels and/or ionized continuum states, core-electron excitation energies of complex molecular system are sensitive first to the chemical changes in local electronic structures around the core-atom of the particular molecule considered[1,2] and second to the spatial coordination and coordination number of surrounding molecules.[3,4] In the case of molecular assemblies such as cluster species, the electrostatic influence of the surrounding molecules on core-hole states and the electronic orbital correlation with the nearest neighboring molecules have turned out to be dominant perturbation factors in the core-electron excitations,[4–6] when intermolecular interaction is significant within the clusters. Among the intermolecular interactions, hydrogen bonding is known to be exclusively the most important interaction[7–11] and often take place between polar organic molecules.

In order to explore spectroscopic details on the H-bonding interaction and structures within the molecular clusters, core-level excitation spectra of H-bonded clusters consisting of simple and polar molecules have been investigated in the supersonic-beam condition[4–6,12–17] using soft x ray radiation sources. The core-excitation spectra of clusters in the beam were extracted without any contribution from molecular excitation by monitoring partial-ion-yields (PIYs) of fragment cations originating from the clusters. In the small cluster regime of beam conditions, quantitative spectral-changes (band shifts and/or band broadenings) as well as qualitative but prominent features of pre-edge excitation structures have been observed in some organic molecules. Specifically, we previously chose small carboxylic acid clusters[4,13,14] as a prototype of strong H-bonded (HB) system in the gas phase, where constituent acid molecules form a stable planar- and cyclic-dimer configuration with doubly bridged (–O−H···O=C<) H-bonds with binding energies of ΔE_b = ca. −65 kJ/mol. Oxygen site-selective core-excitation of the cluster bands of formic acid,[4] for example, showed that the first resonance O $1s_{CO} \rightarrow \pi^*_{CO}$ band shifts upward (to a higher energy) by $\sim$0.31 eV whereas the second O $1s_{OH} \rightarrow \pi^*_{CO}$ band shifts downward by $\sim$0.82 eV rela-

a)Author to whom correspondence should be addressed. Electronic mail: kiyotaba@hiroshima-u.ac.jp.

tive to the monomer bands. The band shifts of the core-to-valence transitions of carboxylic acid clusters have been rationalized primarily by the changes[18] in core-electron binding energies (CEBEs) of the oxygen atoms upon H-bond formation. Very recently, C−H···O(=C) interactions in acetaldehyde (AAL) clusters (with lower hydrogen-donor strength of C−H [Ref. 9]) have been examined at both O 1*s* and C 1*s* pre-edge resonance bands.[5,6,15] In the smallest cluster regime of beam conditions, the most intense O $1s_{HCO} \rightarrow \pi^*_{CO}$ band of AAL clusters was found to shift to a high energy by ~0.15 eV relative to the monomer band. Computer modeling of x ray absorption spectra (XAS) based on the DFT calculation showed that the most stable AAL dimer ($\Delta E_b = -11.3$ kJ/mol at the MP2/cc-pVTZ level) with a non-planar T-shaped geometry could reproduce the experimental cluster band shift. The core-to-valence O $1s_{HCO} \rightarrow \pi^*_{CO}$ band shift was interpreted[5,15] as being both due to the HOMO-LUMO ($n-\pi^*$) interaction and stabilization of the core-hole states,[18] where the current C−H···O interaction was recognized by the appearance of vibrationally blueshifting hydrogen-bonding[11] in the dimer complex. Site-specific band probing in the carbon *K*-edge region[6] was also carried out to analyze the overall molecular configuration within the small AAL clusters since AAL has two different C−H sites (methyl CH_3 and aldehyde CHO (carbonyl) carbon sites) available for the C−H···O interaction. The C 1*s* excitation spectra recorded at a slightly higher stagnation pressure than the above O 1*s* measurement revealed that the intensities of C 1*s* core-to-Rydberg transitions are strongly excitation site dependent upon clusterization, showing the significant reduction of C $1s_{HCO} \rightarrow$ Rydberg bands relative to the monomer bands. Calculated XAS demonstrated that the band reduction appears as a consequence of the site- and geometry-specific C−H···O interaction where planar association between the HCO sites of different AAL molecules becomes significantly important within the small ($n \geq 3$) clusters. The quenching as well as blueshifting of the core-to-Rydberg bands could be rationalized by the anti-bonding σ^*(C−H) character in the Rydberg orbitals of HCO carbon site that may participate through the $n-\sigma^*$ interaction in the weak C−H···O hydrogen bonds.

AM has a simple structure of C_{3V} symmetry with a relatively high dipole moment,[19] comparable to those of typical polar solvents such as water and methanol. Besides, possessed of protic hydrogen atoms and a lone-pair nitrogen site in a molecule, it generally acts as both hydrogen donor and acceptor within the cluster species and constitutes another prototype of H-bonding clusters leading to the formation of HB networks in the condensed systems. Recent theoretical calculations demonstrated that the global minimum of AM dimer[8,20,21] possessed a linearly H-bonded structure with eclipsed *Cs* symmetry and that the stable configurations of small clusters ($n \geq 3$) (Ref. 22) had exclusively simple planer or nearly planer cyclic HB structures; the latter of which may simplify the spectral analysis of core-to-resonance transitions and facilitate the electronic orbital correlation analysis of H-bonded AM clusters. Here, we studied inner-shell excitation and TOF fragment-mass spectroscopies of small AM clusters in the beam conditions, and examined the CEBE changes of the constituent N atoms and the contribution of H-bonding interaction to the cluster core-excitation spectra. The excitation bands of Nitrogen 1*s* core-electrons into the lowest-lying $3sa_1$ and $3pe$ Rydberg orbitals were found to broaden and slightly shift in energy upon cluster formation. These spectral changes of the core-to-resonance excitations found in the small AM clusters are then interpreted using the theoretical DFT calculations.

II. EXPERIMENTS AND THEORETICAL CALCULATIONS

The experiments were carried out using a cluster beam-photoreactive scattering apparatus[23,24] placed behind a varied-line-spacing-monochromator on the soft x ray photochemistry beamline BL-6 of the electron storage ring (HiSOR) at HSRC, Hiroshima University. Continuous $(AM)_n$ cluster beams were generated by supersonic expansion of a gaseous mixture of 10% AM/He through a ϕ 50 μm nozzle under stagnation pressures of $P_0 = 0.15-0.30$ MPa. An "effusive" (monomeric) beam was prepared by the introduction of pure AM gas through a ϕ 200 μm nozzle at a pressure of $P_0 = 11$ kPa. Either beam was doubly collimated with a ϕ1 mm skimmer and a 1×4 mm^2 slit via two differential pumping systems, and finally allowed to enter the main scattering chamber of the apparatus, where it was crossed with a beam of monochromatized soft x rays at the ionization region of a space-focusing TOF fragment-mass spectrometer of Wiley-McLaren type.[25] Electrostatic fields of the TOF spectrometer with a drift length of $L = 300$ mm were chosen so that most of the singly charged ions with kinetic energies up to ~15 eV can be detected without angular discrimination. Photoelectron-photoion coincidence signals were recorded using a fast multihit digitizer with a time resolution typically set to 5 ns. The energy resolution of soft x ray radiation was set to $E/\Delta E = 4000$ at the energy corresponding to the nitrogen *K*-edge. The photon energy was calibrated using the $(N_t\ 1s)/(N_c\ 1s) \rightarrow \pi^*$ transitions of N_2O at 401.13 and 401.73 eV, respectively.[26] Further details have been described elsewhere.[24]

The samples used were of commercial quality. Neat ammonia (NH_3) (purity ≥ 99.999%) and 9.9% NH_3/He mixture in the cylinders were supplied from Taiyo Nippon Sanso Corp.

In order to support the analysis of core-excitation spectra and examine the contribution of H-bonding interactions within the clusters, *ab initio* molecular orbital (MO) and DFT calculations were carried out for AM molecule and clusters. Initial geometries of the system were optimized using the GAUSSIAN 03 program[27] at the MP2/cc-pVTZ level and/or MP2/aug-cc-pVTZ level of approximation. Vibrational frequencies were calculated at the same level to confirm their stationary structures and correct the zero-point vibrational energies (ZPVEs). The frequencies were further scaled[28,29] by multiplying 0.9832 on the MP2 calculations. The basis set superposition errors (BSSEs) were corrected using the procedure proposed by Boys-Bernardi[30] to estimate the plausible stabilization energies of the clusters.

The calculation of core-excited states was carried out with the StoBe-deMon code,[31] based on the solutions of

Kohn-Sham DFT equations. The theoretical XAS were generated using a transition potential (TP) method combined with a double-basis-set technique. The orbital energies and oscillator strengths were calculated to evaluate the transition energies and absorption intensities in the theoretical XAS. The TP method describes most of the relaxation effects on the core-excited states and provides a single set of orthogonal orbitals for the spectrum calculation. In determining the absolute energy positions of the XAS, a ΔKohn−Sham approach[32] that allows full relaxation of ionized core-hole states was performed to derive core-ionization energies (IEs/CEBEs). The relativistic correction of +0.18 eV (Refs. 33 and 34) to the IE of the N 1*s* electrons was made in the present spectral computations. Electron interactions of the nitrogen atoms without any core-electron excitation (core-hole) were described with effective core potentials. Two types of basis sets, the IGLO-III all-electron basis of Kutzelnigg *et al.*[35] and (61111111/41111/111) basis sets, were applied for the description of core-excited nitrogen atoms whereas (311/1) basis set was used for hydrogen atoms. The XAS of AM molecule could be generated by a Gaussian convolution of discrete transition lines by adjusting their broadenings to simulate the experimental spectrum. All DFT calculations were performed using the gradient-corrected exchange (PW86) and correlation functionals (PW91) developed by Perdew and Wang.[36] Further details of the calculations have been given elsewhere.[32,37]

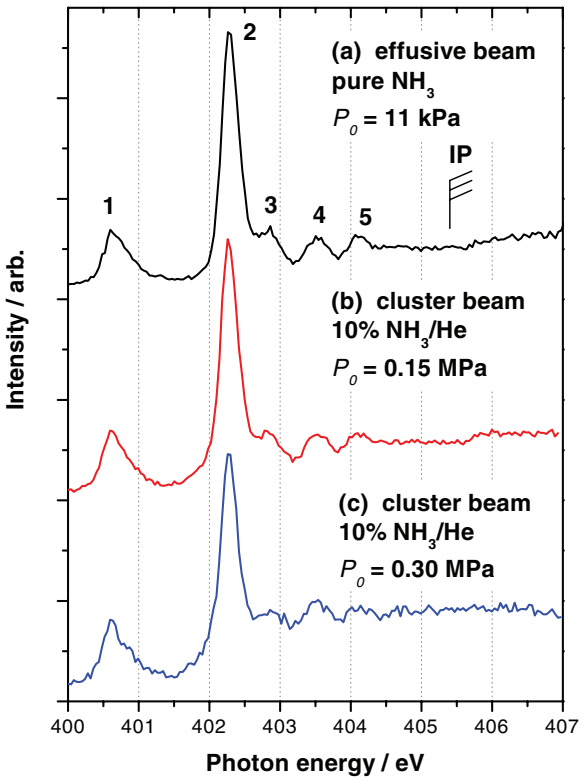

FIG. 1. TIY spectra of ammonia molecule and clusters under the beam conditions designated in the figure, observed with core-excitation at the N *K*-edge region.

III. RESULTS AND DISCUSSION

A. Core-level excitation measurements in the nitrogen *K*-edge region

1. Total-ion-yield spectra of AM molecule and clusters

The top trace in Figure 1(a) shows a typical total-ion-yield (TIY) spectrum of molecular AM in the effusive beam, recorded in the 400−407 eV excitation energy range that covers nitrogen pre-edge transitions. Publications on the x ray absorption and/or excitation spectra of free AM are available in the inner shell electron energy loss spectroscopy (ISEELS) (Ref. 38) and NEXAFS (Ref. 39) measurements. The CEBE of the nitrogen atom in free AM has been determined in the x ray photoelectron spectroscopy.[40] Based on the present band-deconvolution analysis[41] of the free AM peaks and previous assignments,[38,39] we reassigned the results of N 1*s* pre-edge excitation bands as listed in Table I.

Since AM molecule has C_{3V} symmetry, the electronic configuration of occupied orbital in the ground state can be expressed as $1a_1^2 2a_1^2 1e^4\ 3a_1^2$ (X^1A_1). The self-consistent field (SCF) MO calculation showed that the occupied valence orbital, $2a_1$, and doubly degenerated $1e$ are σ(N−H) bonding, whereas the highest occupied $3a_1$ represents the nonbonding n_N (p_Z) orbital on the N atom extending along the principal z axis. The next outer a_1- and e-type-orbitals have actually unoccupied σ^*(N−H) anti-bonding character where they are mixed with the lowest-lying N $1s^{-1}nsa_1$ and N $1s^{-1}np(a_1/e)$ Rydberg states. Two intense TIY peaks in the N 1*s* pre-edge region occur at energies 400.63 (1: N $1s \rightarrow 3sa_1$) and 402.29 eV (2: N $1s \rightarrow 3pe$); relatively broad maxima at 402.76, 403.54, and 404.07 eV below the edge correspond to (3: N $1s \rightarrow 3pa_1$), (4: N $1s \rightarrow 4sa_1$), and (5: N $1s \rightarrow 4p(a_1/e)$) excitations (Table I).

The TIY spectra recorded in the AM cluster beams under stagnation pressures of $P_0 = 0.15-0.30$ MPa are compared in Figures 1(b) and 1(c) (lower traces). The cluster TIY bands have somewhat broader bandwidths and/or band tails with increasing baseline at higher excitation energies. These beam-stagnation conditions are both near the threshold of cluster formation in the small cluster regime.[42] Here, the beams contain significant amounts of uncondensed free AM molecules as well as the clusters of small sizes, so that the production of large-sized clusters is not effectively achieved.

TABLE I. Band-peak assignment of molecular ammonia in the nitrogen *K*-shell region.

	Photon energy (eV)			Term value	
Band no.	Present work	ISEELS[a]	NEXAFS[b]	(eV)	Assignment
1	400.63	400.61	400.66	4.97	$3sa_1$
2	402.29	402.29	402.33	3.31	$3pe$
3	402.76	402.85	402.86	2.84	$3pa_1$
4	403.54	403.52	403.57	2.06	$4sa_1$
5	404.07	404.14	404.15	1.53	$4p$
	(405.60)[c]				*IP*

[a]Sodhi and Brion.[38]
[b]Schirmer *et al.*[39]
[c]Jolly *et al.*[40]

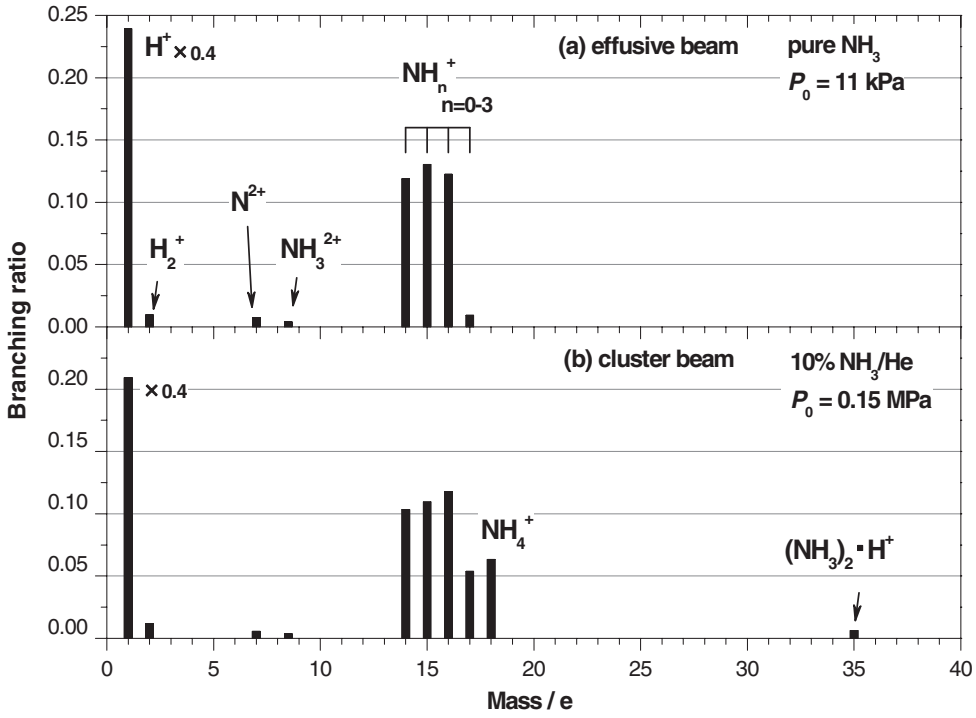

FIG. 2. Comparison of the TOF spectra between (a) the effusive (upper panel) and (b) cluster beams (lower panel), observed with N $1s \rightarrow 3pe$ excitation at 402.3 eV.

2. TOF spectra of AM molecule and clusters

Figure 2 compares (b) a typical TOF spectrum of AM clusters obtained at $P_0 = 0.15$ MPa with (a) that of molecular AM in the effusive beam. Here, the branching ratios of product cations were recorded at the most intense core-excitation band peak (402.3 eV) that corresponds to the N $1s \rightarrow 3pe$ transition. In the effusive beam, one finds intense H^+ and NH_n^+ ($n = 0-2$) but low levels of molecular cation (NH_3^+) and doubly charged products (N^{2+} and NH_3^{2+}). In the cluster beam, we observed the appearance of a series of protonated clusters M_nH^+ ($M = NH_3$), whereas any other production of heterogeneous cluster cations that involve different radical species could not be identified. Interim enhancements of the NH_2^+/NH_3^+ intensities in the fragment masses $m/e \leq 17$ (mass of the parent molecule) were also admitted under low stagnation pressures. These interim enhancements are originated typically from small clusters,[4,13,15] where excess energy transfer following the electronic decays is not necessarily achieved only via molecular evaporation with small energy disposal but sometimes causes subsequent fragmentation steps to give relatively large product cations. It is notable that the protonated clusters M_nH^+ with sizes of $n \leq 3$ at $P_0 = 0.15$ MPa and those with $n \leq 5$ at $P_0 = 0.25$ MPa were detected in the cluster beams, where trace amounts of the maximum-sized M_nH^+ ($n_{max} = 3$ and 5) were identified. Atomic and smaller fragments such as H^+, H_2^+, N^+, and NH^+ in the cluster beam show relative TOF-intensity patterns similar to that of the effusive beam, it is thus reasonable to postulate that they are substantially of free AM origin since the cluster beam produced under the stagnation condition in Figure 2(b) is considered to involve a fair amount of uncondensed free molecules.

3. Partial-ion-yield spectra of AM clusters

Figure 3 compares the PIY spectra in the 400−403 eV excitation energy region for the monomer- and cluster-origin cations simultaneously recorded at the same energy points. The atomic and small fragment cations from free AM molecule actually showed almost the same PIY peak positions (Figure 3(a)) as those of the TIY bands (top traces of Figure 3) in the effusive beam, when the PIY peaks were determined with the aid of deconvolution analysis. In contrast, the PIYs of the cluster-specific products, M_nH^+ (and NH_3^+) have different characteristics of the resonance peaks from the TIY bands in the effusive beam; the cluster N $1s \rightarrow 3sa_1/3pe$ peaks are found definitely broaden and slightly shift, as a whole, to a low-energy side by a few tens of a meV. Table II lists the band broadenings for the lowest-lying N $1s \rightarrow 3sa_1/3pe$ transitions obtained under stagnation pressures of 0.15 and 0.25 MPa (Figures 3(a) and 3(b)), where FWHMs of the corresponding bands are indicated. Here, the lowest stagnation pressure was chosen so as to obtain a small cluster-sized distribution as possible under the beam conditions that the point-by-point signal accumulation can be made in the cluster PIY measurement. While the band broadening of the N $1s \rightarrow 3sa_1$ transition was found to be ΔFWHM = ~0.2 eV relative to the molecular case, rather significant broadening of ΔFWHM = ~0.5 eV could be identified for the N $1s \rightarrow 3pe$ cluster band. These band broadenings are probably due to the contributions from both the splitting of degenerate core-excited states and the

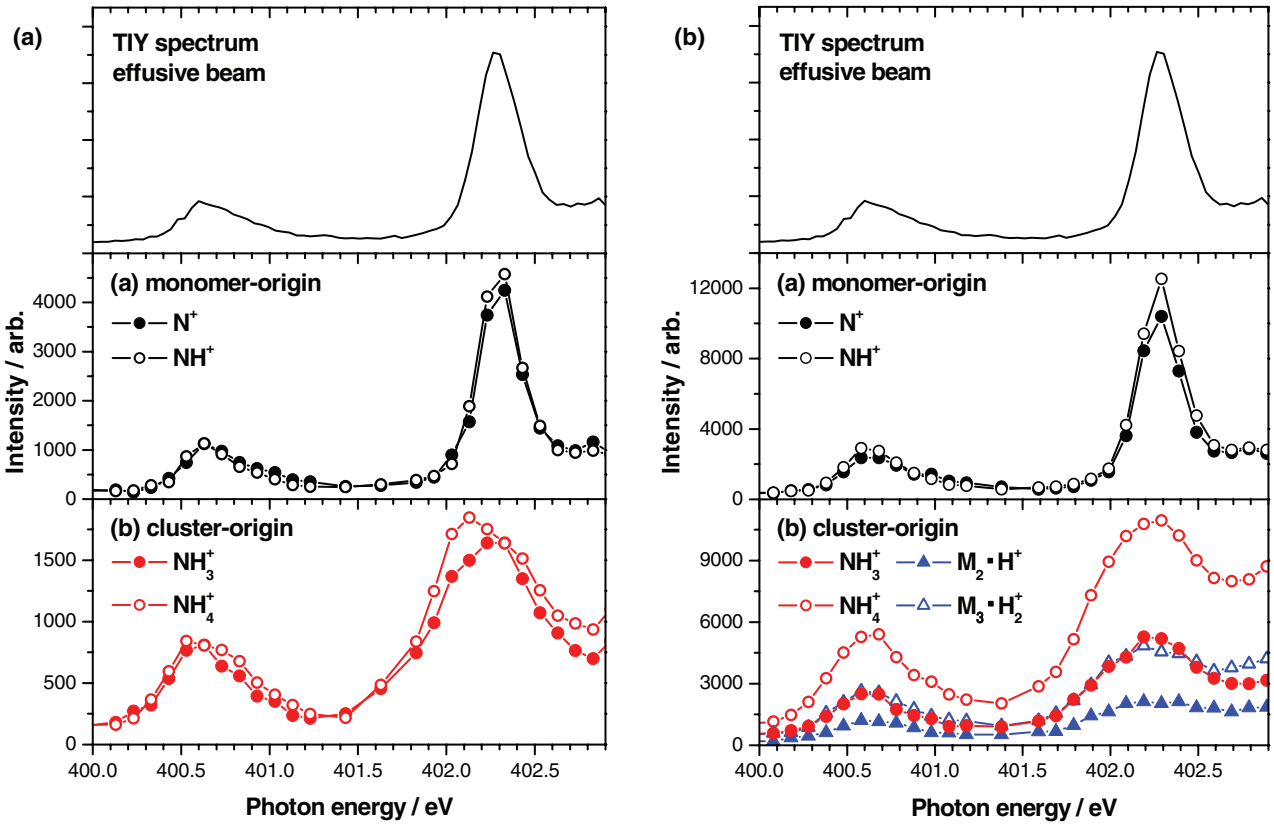

FIG. 3. Comparison of the PIY spectra for some representative cations, N^+, NH^+, NH_3^+, and NH_4^+ at the N $1s \rightarrow 3sa_1/3pe$ transitions, observed in the different cluster beams. (a) $P_0 = 0.15$ MPa; (b) $P_0 = 0.25$ MPa. The TIY spectrum of molecular ammonia is also shown at the top panel.

appearance of transitions for $(AM)_n$ clusters of different sizes and isomers. It should be added here that the spectral difference in the PIYs between NH_3^+ and NH_4^+ (exact peak position of the second NH_3^+ band in Figure 2) is mostly due to the contribution of free molecules since a very small amount of the NH_3^+ product comes from free molecules as described above.

B. Comparison of experimental spectra with XAS generated by DFT calculations

1. Structures and binding energies of small AM clusters

The structure of AM dimer complex has a very flat potential energy surface in the region connecting the linear and cyclic configurations, and has been a continuous subject of investigations for the last two decades.[8] Theoretical calculations[20] with high levels of basis set and proper inclusion of electron correlation showed that the global minimum of AM dimer was characterized as a linearly eclipsed (*Cs*) H-bonded structure (Figure 4(a1)) rather than the corresponding staggered (*Cs*: Figure 4(a2)) or doubly H-bonded cyclic (C_{2h}: Figure 4(a3)) structures. Recent calculations claimed[21] that the latter cyclic structure is a saddle point corresponding to the interconversion between the proton donor and acceptor moieties with a barrier height around ~200 J/mol.[43] The energy difference between the linear and cyclic structures is so small that the inclusion of BSSE correction makes them almost identical; the MP2 complete basis set (CBS) limits[44] of their binding energies were calculated to be around $\Delta E_b = -13.0$ kJ/mol.[20] Further ZPVE correction was included for the eclipsed *Cs* dimer structure, then the binding energy of $\Delta E_b = -6.79$ kJ/mol (Ref. 21) has been derived at the MP2/aug-cc-pVTZ level. Our *ab initio* MO calculation of the eclipsed *Cs* dimer leaded $\Delta E_b = -6.78$ kJ/mol with ZPVE correction at the level of MP2/CBS limit.

TABLE II. The bandwidths of the first two resonance transitions observed in the PIY spectra for the monomer- and cluster-origin products.

	Excitation	FWHM (eV)		
P_0 (MPa)	Band	Cluster-origin	Monomer-origin	ΔFWHM (eV)
0.15	N $1s \rightarrow 3sa_1$	0.53 ± 0.05	0.38 ± 0.06	+0.15
0.15	N $1s \rightarrow 3pe$	0.78 ± 0.06	0.29 ± 0.02	+0.49
0.25	N $1s \rightarrow 3sa_1$	0.52 ± 0.03	0.31 ± 0.00	+0.21
0.25	N $1s \rightarrow 3pe$	0.75 ± 0.03	0.31 ± 0.00	+0.49

For the structures of neutral clusters larger than the dimers, *ab initio* MO studies supporting the experimental findings have also been reported.[22,45] The most stable configurations of the trimer and tetramer were found to have planar or nearly planar cyclic structures of H-bonds with C_{3h} and C_{4h}/D_{4h} symmetries. For larger clusters than the pentamer,[45] three-dimensional structures with increasing tendency to the amorphous have also been predicted. The examples of the most stable structures for C_{3h} trimer and C_{4h} tetramer chosen for the present study are shown in Figure 4(b)–4(e),

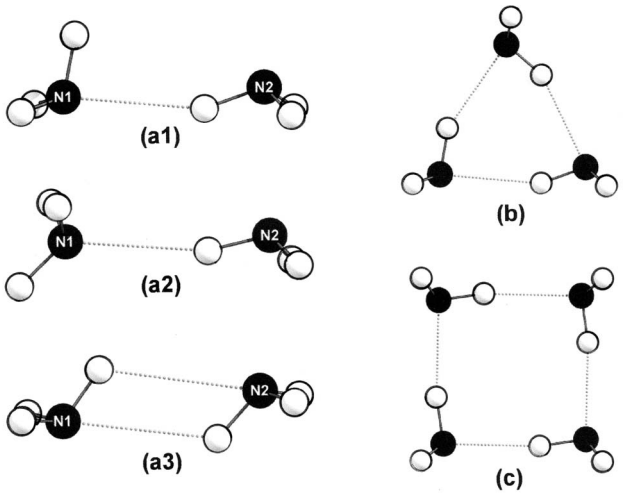

FIG. 4. Examples of the representative configurations optimized for AM dimers and the most stable $(AM)_n$, $n = 3-4$ clusters.

where they are optimized at the MP2/aug-cc-pVTZ level. Their complexation energies were calculated here as $\Delta E_b = -28.0$ kJ/mol for C_{3h} trimer and $\Delta E_b = -44.8$ kJ/mol for C_{4h} tetramer, including the BSSE and ZPVE corrections.

2. X-ray absorption spectra by DFT calculation

In order to give an interpretation for the band shift and/or band broadening of the cluster-specific excitation spectra in the N *K*-edge region, model XAS were generated for the representative AM clusters of small sizes using the DFT calculation,[31] since the cluster bands were recorded under the small cluster regime of beam conditions. The most stable structure of eclipsed *Cs* dimer optimized at the MP2/aug-cc-pVTZ level is shown in Figure 4(al), where the atoms that constitute the N1···H−N2 hydrogen bond are located on a σ_h mirror plane. Table III lists the calculated H-bond (N−H···N) parameters of eclipsed *Cs* dimer and its core-ionization energies (CEBEs) from the individual N 1*s* orbitals. The N1···H length of *Cs* dimer is around ∼2.3 Å that shows less than the sum (2.75 Å) of van der Waals radii[46] of nitrogen and hydrogen (vdW cutoff), the AM molecules being definitely associated by the H-bonding interaction.

Figure 5 compares the XAS of the N $1s \rightarrow 3sa_1/3pe$ transitions between (a) free AM molecule and (b) the most

TABLE III. Hydrogen-bond parameters and CEBEs of small ammonia clusters.

Cluster	Core-atom	$d_{NH\text{-}N}$[a] (Å)	$\theta_{NH\text{-}\cdot N}$[a] (deg)	ΔCEBE[b] (eV)
Dimer (*Cs*)	N1 (H-acceptor)	2.282	155.4	+0.128
	N2 (H-donor)			−0.914
Trimer (C_{3h})	N (donor/ acceptor)	2.212	155.3	−0.837
Tetramer (C_{4h})	N (donor/ acceptor)	2.134	170.6	−1.069

[a]Calculated at MP2/aug-cc-pVTZ.
[b]CEBE of ammonia molecule by DFT calculation is 405.96 eV.

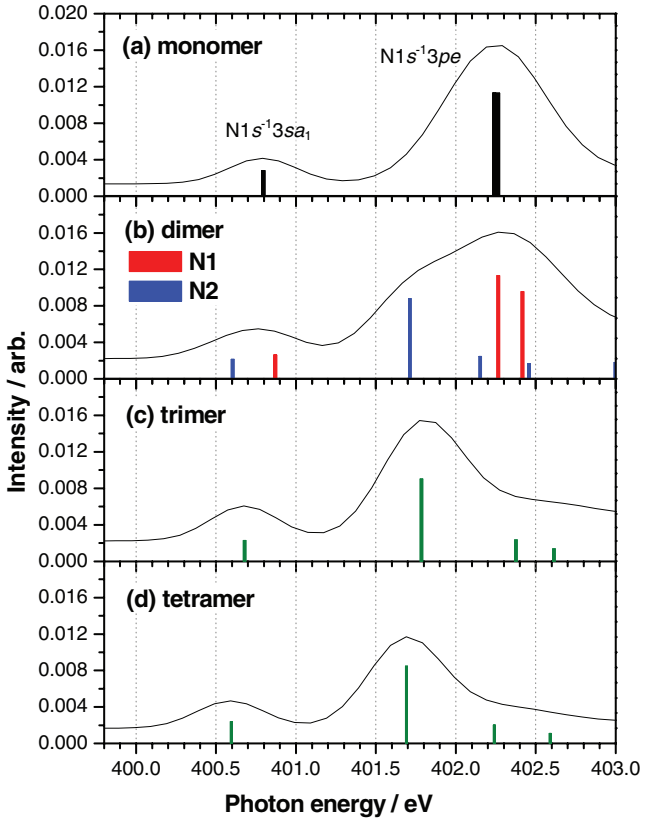

FIG. 5. Comparison of the calculated N $1s \rightarrow 3sa_1/3pe$ band spectra among AM molecule and the most stable $(AM)_n$ clusters. The vertical bar denotes the oscillator strength of the N 1*s* transition at the corresponding energy position.

stable *Cs* dimer, calculated with the DFT formalism (we designate hereafter the states and transitions of clusters as those corresponding to AM monomer). The vertical (colored) bars represent the oscillator strengths of individual transitions from the constituent N atoms in *Cs* dimer (Figure 5(b)). Since two nitrogen atoms become inequivalent under their chemical surroundings, their excitation energies as well as CEBEs split into two different components from that in free molecule by coupling with both the overall intermolecular electrostatic interaction[18] and local inter-nuclear interaction such as the H-bonding. A stable dipole-dipole configuration (e.g., Figures 4(a1)–4(a3)) of neutral dimer occasionally induces a strong monopole (point charge) dipole interaction upon core-electron ionization and then increases and/or decreases the CEBE (Ref. 5) in addition to the H-bonding interaction, when it is compared with the CEBE value of free molecule. In the present *Cs* dimer configuration, less stable core-ionization state (ΔCEBE = +0.13 eV) for the H-acceptor N1 atom[47] and much more stable core-ionization state (ΔCEBE = −0.91 eV) for the H-donor N2 atom[48] than that of free molecule have been calculated (Table III). The gross magnitudes of the change in the core-ionization energies could be explained with a simple approximation of the charge-dipole interaction,[5] in the previous work on AAL dimers. The change in the CEBE for each N atom in *Cs* dimer was checked here by the intermolecular point charge multipole interaction using the SCF (i.e., Hartree-Fock) level of *ab initio* MO approximation.[27] Most of the difference

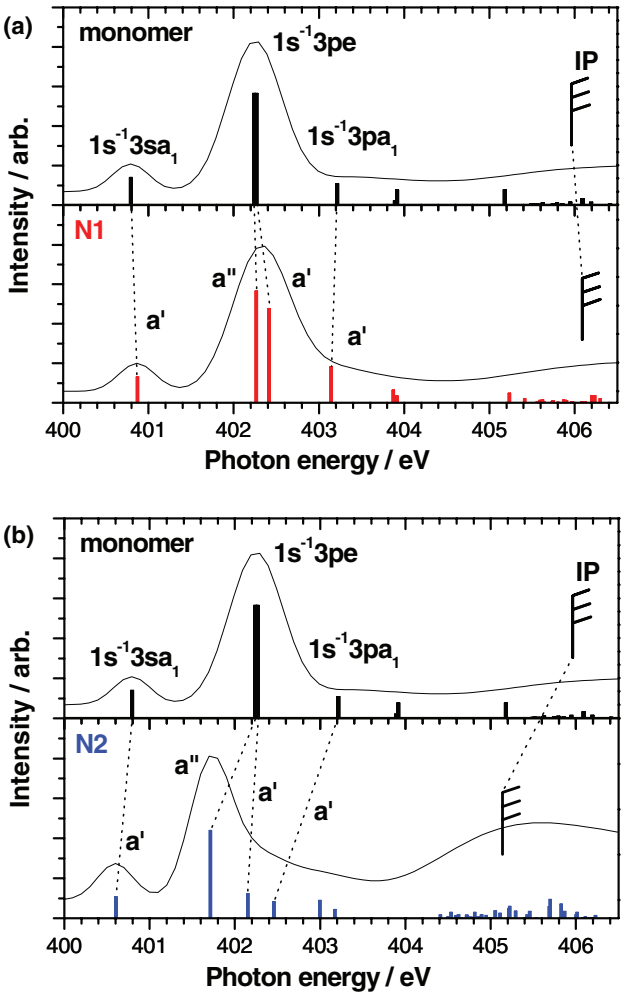

FIG. 6. Comparison of the calculated N $1s \rightarrow 3sa_1/3pe/3pa_1$ transitions of *Cs* dimer with those of AM molecule. Excitations of the inequivalent N atoms in the dimer are indicated. (a) Core-electron excitations of N1 atom. (b) Core-electron excitation of N2 atom.

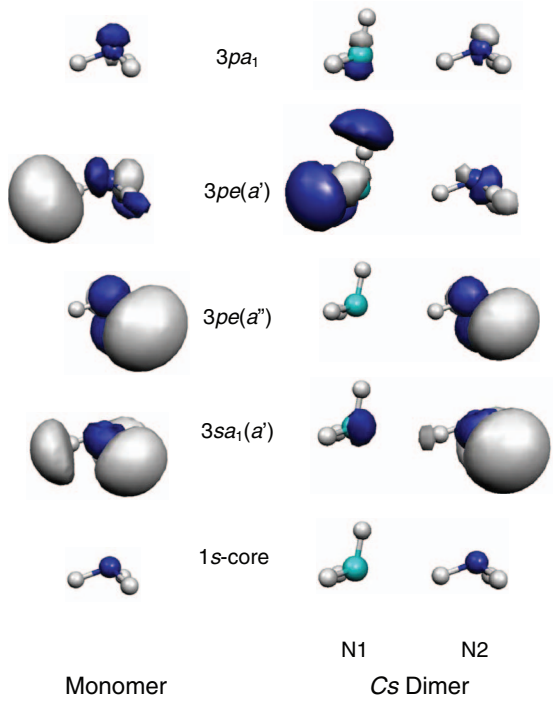

FIG. 7. Molecular orbitals showing the lowest-lying excited $3sa_1/3pe/3pa_1$ states of molecular AM and those of the most stable AM dimer (*Cs*). The MOs associated with the N2-site excitation are indicated for *Cs* dimer.

(0.82 eV) in the CEBEs of the N atoms (Table III) is well interpreted as being due to such electrostatic intermolecular core-hole interaction.[18] A similar trend for the excitation energy by the charge-multipole interaction is more or less expected in each of the core-to-Rydberg states. The nitrogen atoms in the planar cyclic trimer and tetramer, which we chose here as one of the representatives for the most stable clusters of small sizes, are all equivalent within the system under the C_{3h} and C_{4h} symmetry (with the same H-donor and H-acceptor configuration) so that their excitation energies are actually degenerate (Figures 5(c) and 5(d)). Table III also lists the molecular parameters (N···H–N) around the N atoms to be core excited and their core-ionization energies for these representative C_{3h} and C_{4h} clusters.

2.1. Lowest-lying core-to-Rydberg transitions of the most stable Cs dimer. In Figure 6, the XAS (Figure 5(b)) calculated for *Cs* dimer was separated into two component spectra made up of individual Nl and N2 core-electron excitations. To obtain a deeper understanding of orbital correlations within the complex, the molecular orbitals associated with the molecular excitation of AM and N2 excitation of *Cs* dimer are also shown in Figure 7, where the N 1*s* core and the lowest-lying Rydbergs of the N2 excitation, $3sa_1(a')$, $3pe(a'/a'')$, and $3pa_1(a')$ orbitals are given (MOs of the N1 excitation of *Cs* dimer are not shown here). Since the H-bonding in the present dimer system occurs only via the lone-pair orbital singly on the N1 atom, interaction with the orbitals (associated with the σ/σ^*(N−H) character) on the N2 atom in the counter molecule are exclusively important (N2-type interaction). Core-excited orbitals on the N1 (H-acceptor site) are thus mostly free from the H-bonding of the in-plane N1···H−N2 structure, demonstrating the transition patterns (N1-type interaction) similar to the unperturbed molecular ones (Figure 6(a)). As described above, the core-to-Rydberg excited states of N1 are more or less affected simply by the intermolecular core-hole interaction as the core-ionization state is. The small splitting appeared in the N1[N$(1s)^{-1}3pe$] states shown in Figure 6(a) can be attributed to a further weak through-space (π^* anti-bonding) interaction between the N1[$3pe(a')$] and N2[$3a_1$(lone-pair)] orbitals.

In contrast, the effects of H-bonding interaction on the core-to-Rydberg states strongly appear in the N2 excitation site (Figure 6(b)), namely in the N–H (H-donor) site. The intermolecular core-hole interaction (results in the change in CEBE) of the N2 site in *Cs* dimer configuration first stabilizes the core-to-Rydberg excited states of the N2 atom. The N2[N$(1s)^{-1}3pe(a'')$] orbital shown in Figure 6(b) is totally irrelevant to the H-bonding upon dimerization due to the out-of-plane character against the σ_h (xy) mirror plane. The significant redshift of the N2[N$(1s)^{-1}3pe(a'')$] transition is thus

attributed simply to the stabilization of the N2 core-excited states by the core-hole interaction. A similar situation to the above occurs in the N2[N($1s$)$^{-1}3pa_1(a')$] transition where the $3pa_1(a')$ orbital on N2 is expanding along the y axis mostly perpendicular to the N1···H−N2 hydrogen bond, despite the in-plane a' symmetry, leading to another highly redshifting transition. The other lowest-lying N2 core-to-Rydberg transitions, N2[N($1s$)$^{-1}3sa_1(a')$] and N2[N($1s$)$^{-1}3pe(a')$] involve the H-bonding interactions with the σ*(N−H) character in their excited orbitals, in addition to the core-hole interaction. When the H-bonding of the N1···H−N2 takes place, relevant MOs (occupied states) associated with the n non-bonding and σ(N−H) bondings are stabilized whereas those with σ*(N−H) anti-bonding (vacant states) become instable depending on the magnitudes in its matrix elements of the interaction. In the case of N2 core-excitation to the Rydberg states in *Cs* dimer, the H-bonding and core-hole interactions exert their effects on the orbital energies in the opposite direction and result in smaller redshifts of the excitation energy when the excited state are associated with the H-bonding, since the magnitude of the present core-hole interaction is larger than that of the H-bonding. As the first excited N2[N($1s$)$^{-1}3sa_1(a')$] has actually an s-type orbital in nature, the matrix element of the interaction may be rather weak among the anti-bondings on N2 with the a' symmetry. In Figure 7, one can realize the mixings of the originating orbitals in the N2[N($1s$)$^{-1}3sa_1(a')$] and N2[N($1s$)$^{-1}3pe(a')$] states; the $3sa_1(a')$ orbital on the N2 atom correlates with the lone-pair $3a_1$ on the N1 atom in the N2[N($1s$)$^{-1}3sa_1(a')$] state, and the $3pe(a')$ orbital is mixing with the $3sa_1$ of the same a_1 symmetry in the N2[N($1s$)$^{-1}3pe(a')$] state. These excited states with the σ*(N−H) anti-bonding components are perturbed (by the $n \rightarrow \sigma^*$ interaction) upon H-bonding formation and destabilizes their orbital energies[10,14] via the production of additional anti-bonding structures between the associated molecules. The potential energy changes in the relevant excited states thus far described in the present paragraph, are also summarized in Figure 8.

Expansion of the excited orbital to the counter molecule(s) implies that electron transfer from the core-excited molecule to the counter molecule(s) is taking place and that electron density in the core molecule delocalizes over to the counter molecule(s) upon complexation. The reduction of oscillator strength for the N2 excitation to the [N($1s$)$^{-1}3pe(a')$] relative to the free molecule can thus be attributed to the significant decrease in Franck-Condon density by the delocalization of MO via the interaction of the H-bonding. Excited MOs insensitive to the H-bonding interaction provide the oscillator strengths similar to those of the molecular excitation. The core-excitation to the N2[N($1s$)$^{-1}3pe(a'')$] state shows a typical transition to preserve its high oscillator strength upon H-bond formation. As the consequence of these H-bonding interaction and core-hole interaction, the structures (splitting and energy shift) of the core-to-Rydberg transitions of *Cs* dimer could be interpreted. The XAS calculation of *Cs* dimer shows that the N1–N2 splitting of the [N($1s$)$^{-1}3sa_1$] band energy is ∼0.27 eV, and the most intense a'' component of the transition in the [N($1s$)$^{-1}3pe$] band shows the N1–N2 splitting of ∼0.56 eV

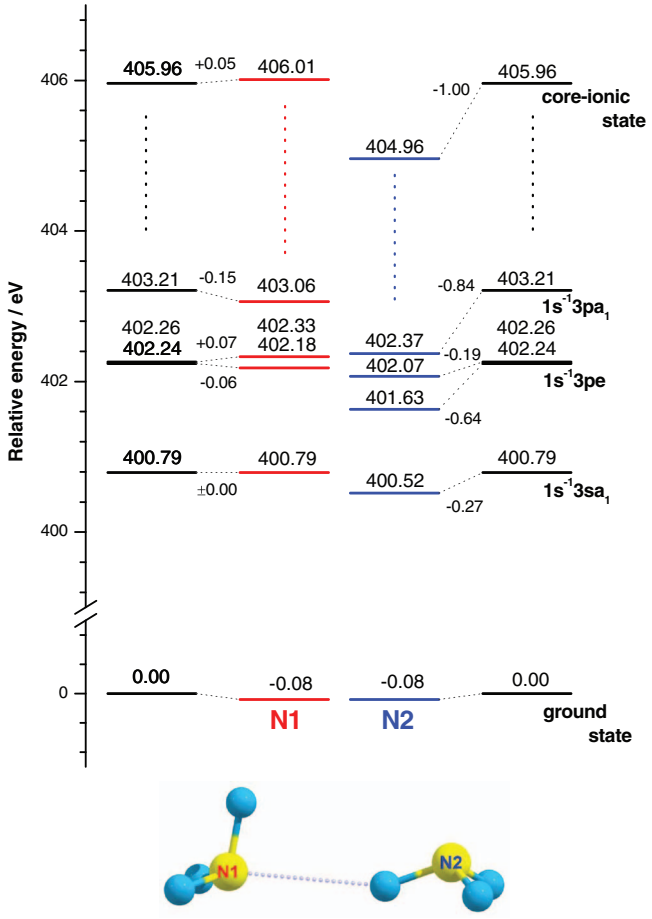

FIG. 8. Energy level diagram for the core-excited states of individual N atoms in the most stable *Cs* dimer. Energy levels of molecular AM are also shown for comparison.

while the splitting of the a' component gives a value of ∼0.27 eV.

2.2. Lowest-lying core-to-Rydberg transitions of the most stable trimer and tetramer. In the preceding section, it has been shown that the intermolecular core-hole interaction is first important to define the overall stabilities for the core-to-Rydberg excitation states. The H-bonding interaction, in contrast, is sensitive to the exact nature of the H-bond donor/acceptor structure and exclusively depends on their orbital correlations within the configuration. The changes in the XAS of the complex system are predominantly the outcome of these two interactions. In the XAS of the most stable *Cs* dimer, a terminal NH_3 molecule with three free N−H bonds (N1-type interaction of a pure acceptor configuration) shows the core-to-Rydberg transition structures mostly similar to the free NH_3 molecule, since it involves least active MOs other than the occupied lone-pair (n) for the H-bonding. The AM molecule with an H−N donor configuration and two free N−H bonds (N2-type interaction) has several lowest-lying Rydberg orbitals that involve the components of σ*(N−H) character, leading to the shifting and splitting of the core-to-Rydberg transitions accordingly to higher energies. In what follows, the core-excited states of the N atoms in cyclic AM

clusters are governed only by the N2-type interaction since the terminal acceptor molecule(s) with three free N−H bonds is (are) not involved.

In Figures 5(b) and 5(c), the XAS of the representative C_{3h} trimer (Figure 4(b)) in the lowest-lying Rydberg region can be compared with that obtained in the *C*s dimer case. Here, the N atoms to be core-excited in C_{3h} trimer are all equivalent under their chemical surroundings, each being possessed of the N2-type configuration. Based on the H-bonding geometry considerations, the level of H-bond strength is empirically characterized by an H-bond distance d(N−H···N) and its donor directionality θ (N–H···N). The true H-bond nature of the interaction favors a linear N−H···N structure ($\theta \sim 180^\circ$) with a shorter N−H···N distance than the vdW cutoff (2.75 Å). The comparison of these H-bond parameters between C_{3h} trimer and *C*s dimer in Table III shows that the H-bond distances are mostly comparable with each other under the same donor directionality. One may thus postulate that almost the same level of H-bond interaction in the individual N−H···H as that in *C*s dimer takes place within C_{3h} trimer. In addition to the geometry considerations, each N core-atom in the trimer is also found to have a lower magnitude of CEBE (Table III) than free molecule but comparable to the N2 atom in the *C*s dimer case, again indicative of a similar level of core-hole interaction. Under such circumstances, it is thus natural that the cyclic trimer with C_{3h} symmetry shows a spectral pattern similar to the case of the N2-type interaction (Figure 5(b)), although the transitions designated are triply degenerate. The core-to-Rydberg transitions of the cyclic trimer constitute the corresponding $3sa_1$ band shifting to a lower energy by ∼0.11 eV and the intense component *a*" of the corresponding 3*pe* band that appears at an energy position lower by ∼0.47 eV than the free molecule.

In the planar cyclic AM clusters, N 1*s* core-excitation spectra are actually governed by the N2-type interaction, although each band is multiple degenerated as the case of C_{3h} trimer. The XAS derived for C_{4h} tetramer is also compared with each other (Figure 5(d)). Since the angle formed by the N−H and lone-pair axes of an isolated AM molecule is ∼112°, the most favorable H-bond geometry could be expected in the cyclic pentamer (and/or hexamer) with interior angles of ∼108°−120°. In fact, shorter H-bond distances ($d_{\mathrm{NH\cdots N}} = 2.10-2.11$ Å) and better donor directionalities ($\theta_{\mathrm{NH\cdots N}} = 173^\circ-176^\circ$) than the C_{3h} trimer are derived at the same level of MP2 calculation, despite being non-planar cyclic pentamers and hexamers. As far as the H-bonding geometry consideration on C_{4h} tetramer is concerned, it is reasonable to postulate that the $d_{\mathrm{NH\cdots N}}/\theta_{\mathrm{NH\cdots N}}$ parameters as listed in Table III are thus very close to the most favorable ones for the H-bonding interaction. The cluster CEBEs of constituent N atoms (Table III) derived from the present DFT calculation, in turn, decrease by ∼0.2 eV as the cluster size increases from C_{3h} trimer to C_{4h} tetramer. Such gradual stabilization of cluster core-ionization states has also been predicted in the H-bonded $(H_2O)_n$ clusters,[49] where an asymptotic lowering of the CEBE to the experimentally observed level (ΔCEBE = −1.1 eV at a cluster size of $n = 20$) was identified. In addition to the aforementioned features of the CEBE dependences on donor/acceptor configuration (in *Cs* dimer) and on the cluster size, the stabilization energies (ΔCEBEs) evaluated in AM clusters have the magnitudes similar to the $(H_2O)_n$ case. Although the core-excitation of clusters correlates with both the intermolecular core-hole (CEBE changes) and local H-bonding interactions at a corresponding core-site within the cluster, a larger increment in the stability (ΔCEBE) than that in the $n-\sigma^*$ instability actually governs the energy shift of the core-to-Rydberg transitions. The overall spectral shifts of the C_{4h} bands (Figure 5(d)) to lower energies are thus interpretable relative to the C_{3h} trimer. Spectral DFT calculation of C_{4h} tetramer showed that the first core-excitation to the corresponding $3sa_1$ Rydberg band shifts to a lower energy by ∼0.19 eV, and that the intense component *a*" of the second 3*pe* band appears at an energy position lower by ∼0.56 eV than the free molecule.

3. Comparison between cluster-specific PIYs and theoretical XAS

The PIY spectra were measured by monitoring the cluster-specific product, $(NH_3)_nH^+$ (and NH_3^+) at stagnation pressures $P_0 = 0.15-0.25$ MPa. The lower pressure limit was employed to provide cluster-size distribution as small as possible for the plausible PIY spectrum under the stable cluster-beam conditions. At the onset of small cluster regime of beam condition, an exponential intensity decrease with cluster size n is generally observed. The cluster size distribution then shifts to larger clusters with increasing stagnation pressure (i.e., increasing condensation parameter Γ^* (Ref. 42) and gradual contribution of larger clusters could be expected to the observed PIYs. Since the present PIYs obtained at the different beam conditions are mostly similar in their band features (Table II), where the beam conditions are near the threshold of AM-cluster formation, it is natural to assume that $(AM)_n$ with the smallest size distributions may contribute significantly to the present PIY spectra. One may thus recognize that the computer modeling of the major $(AM)_n$ ($n \leq 4$) clusters is actually appropriate for the interpretation of band broadenings appeared at the core-to-Rydberg bands.

The first cluster band, core-to-$3sa_1$ Rydberg transition actually reflects a weaker H-bond interaction via a small σ^*(N−H) character involved, and has a relatively small oscillator strength as the molecular N $1s^{-1}3sa_1$ band shows. The distinct characteristics of the intermolecular interactions strongly appear in the change of the second N $1s^{-1}3pe/3pa_1$ band. In the case of the representative *C*s dimer (Figure 8), N2 core-excitation shows the $3pe/3pa_1$ transitions highly characteristic of the structure of H-bonding cluster-band; it totally causes significant redshifts of the $3pe(a'')/3pa_1$ components (as opposed to N1 core-excitation) via the core-hole interaction that result in the splitting of core-excited N1/N2 levels to lead substantial broadening of the second core-to-Rydberg band. As the N1 excitations with higher-energy components, however, are close to the monomer ones, least H-bonding and less core-hole interactions on the acceptor N1 could be inferred from the structures of the N1 core-to-Rydberg transitions. The band splitting of *C*s dimer, $\mathrm{SP[N}(1s)^{-1}3sa_1/3pe] = [0.27\ \mathrm{eV}/0.56\ \mathrm{eV}]$ are found very close to the increments for the experimental band broadenings

ΔFWHM(N(1*s*)$^{-1}$3*sa*$_1$/3*pe*) = [0.15−0.21 eV/0.49 eV]. In contrast, C_{3h} trimer has three equivalent N core-atoms with the same levels of the H-bonding and CEBEs as the N2-type in *C*s dimer, showing the transition structures in a similar manner to the N2 excitation. Possessed of stronger H-bonds and lower CEBEs, C_{4h} tetramer totally shifts their 4-fold components of the N(1*s*)$^{-1}$3*sa*$_1$/3*pe* transitions to slightly lower energy positions than the C_{3h} trimer. The theoretical core-to-Rydberg bands of cyclic clusters simply show the energy shifts to lower energies by 0.11–0.19 eV at the N(1*s*)$^{-1}$3*sa*$_1$ and by 0.47–0.56 eV at N(1*s*)$^{-1}$3*pe* transitions, relative to the monomer bands. Summarizing the comparison of the changes in cluster bands (Table II) with those calculated, the magnitudes of the experimental broadening in 3*sa*$_1$ (0.15–0.21 eV) and 3*pe* bands (∼0.49 eV) are found as large as the shifts and/or splittings of these representative clusters in the present DFT calculations. The band broadening of AM clusters could thus be rationalized by the shift and splitting of the core-electron excitations involved in the constituent H-bonded molecules.

The cluster beam being made of the mixtures of clusters with small sizes, the PIY spectra are regarded as those composed of these constituent clusters. The high-energy sides of the experimental 3*sa*$_1$/3*pe* band structures are only accounted for by the N1 components of *C*s dimer, whereas larger clusters with cyclic structures exclusively play an important part to constitute the low-energy sides of the experimental cluster bands, in addition to the N2 components of *C*s dimer. Under the small cluster regime of beam conditions, we thus conclude that the stable *C*s dimer is present in the highest concentrations and the presence of cyclic clusters of trimer/tetramer is of secondary importance to account for the broadenings of the lowest-lying core-to-Rydberg cluster-bands. Since the center of gravity for the experimental second cluster-band (3*pe*/3*pa*$_1$) clearly appears at a lower energy position than the monomer band, subsidiary contribution of the cyclic clusters (at first of the C_{3h} trimer) is necessitated by the basic XAS of *C*s dimer to reproduce the experimental core-to-Rydberg cluster-bands.

IV. CONCLUSIONS

N l*s* core-electron excitation spectra of ammonia clusters have been studied in the small cluster regime of beam conditions. Pre-edge resonance bands of the small clusters revealed that the first resonance bands of N 1*s* → 3*sa*$_1$/3*pe* are considerably broadened relative to the free molecule. The band broadening of the lowest-lying Rydberg N 1*s* → 3*sa*$_1$ transition was found to be ΔFWHM = ∼0.20 eV whereas rather significant broadening of ΔFWHM = ∼0.50 eV could be identified for the second N 1*s* → 3*pe* Rydberg bands. The density functional theory calculation was applied to rationalize these experimental results. Based on the geometrical optimization using *ab initio* MO calculation, the most stable eclipsed (*Cs*) dimer, planar cyclic trimer (C_{3h}) and tetramer (C_{4h}) were chosen as the representatives of small clusters with stable configurations, and subjected to the spectral simulation of the lowest-lying N 1*s* → 3*sa*$_1$/3*pe* transitions. The spectral simulation has found that the site-dependent CEBE governed by the intermolecular core-hole interaction is primarily important to define the overall stabilities for the core-electron excited states. The H-bonding interaction is sensitive to the exact nature of the H-bond donor structure and exclusively depends on their orbital correlation within the molecular configuration of the system. The molecule with an H−N donor configuration in the cluster system has several lowest-lying Rydberg orbitals that involve the components of σ*(N−H) character for the H-bonding interaction, leading to the shifting of the core-to-Rydberg transitions accordingly to higher energies. The spectral changes (band shifts and/or band broadenings) in these complex systems are mostly outcomes of these two interactions. The simulation of the most stable eclipsed dimer (*Cs*) could reproduce most of the characteristic features for the experimental N 1*s* → 3*sa*$_1$/3*pe* band broadening upon clusterization, showing a significant contribution of *Cs* dimer in the small cluster regime of beam conditions.

ACKNOWLEDGMENTS

The present study was performed under the Cooperative Research Program (Nos. #07-A-58 and #08-A-51) of HiSOR, at HSRC, Hiroshima University. The present work was partly supported by a grant-in-aid for scientific research (B) from the MEXT (Grant No. 21350014). One of the authors, K. Tabayashi thanks the Research Center for Computational Science at the Okazaki Research Facilities of the Japanese National Institutes of Natural Sciences, for the allocation of SGI Altix4700 computer time. O. Takahashi is grateful for the financial support from a grant-in-aid for scientific research from JSPS of Japan (Grant No. 23540476).

[1] J. Stöhr, *NEXAFS Spectroscopy*, Springer Series in Surface Science Vol. 25 (Springer, Berlin, 1992).
[2] Ph. Wernet, D. Nordlund, U. Bergmann, M. Cavalleri, M. Odelius, H. Ogasawara, L. Å. Näslund, T. K. Hirsch, L. Ojamäe, L. G. M. Pettersson, and A. Nilsson, Science **304**, 994 (2004).
[3] E. Rühl, Int. J. Mass Spectrom. **229**, 117 (2003).
[4] K. Tabayashi, K. Yamamoto, O. Takahashi, Y. Tamenori, R. Harries, T. Gejo, M. Iseda, T. Tamura, K. Honma, I. H. Suzuki, S. Nagaoka, and T. Ibuki, J. Chem. Phys. **125**, 194307 (2006).
[5] K. Tabayashi, M. Chohda, T. Yamanaka, Y. Tsutsumi, O. Takahashi, H. Yoshida, and M. Taniguchi, J. Phys. Conf. Ser. **235**, 012017 (2010).
[6] K. Tabayashi, Y. Tsutsumi, M. Chohda, O. Takahashi, Y. Tamenori, I. Higuchi, I. H. Suzuki, S. Nagaoka, T. Gejo, and K. Honma, J. Phys. Conf. Ser. **288**, 012022 (2011).
[7] L. A. Curtiss and M. Blander, Chem. Rev. **88**, 827 (1988).
[8] S. Scheiner, *Hydrogen Bonding* (Oxford University Press, Oxford, 1997).
[9] G. A. Jeffrey, *An Introduction to Hydrogen Bonding* (Oxford University Press, Oxford, 1997).
[10] A. E. Reed, F. Weinhold, L. A. Curtiss, and D. J. Pochatko, J. Chem. Phys. **84**, 5687 (1986).
[11] P. Hobza and Z. Havlas, Chem. Rev. **100**, 4253 (2000).
[12] O. Björneholm, F. Federmann, S. Kakar, and T. Möller, J. Chem. Phys. **111**, 546 (1999).
[13] K. Tabayashi, K. Yamamoto, T. Maruyama, H. Yoshida, K. Okada, Y. Tamenori, I. H. Suzuki, T. Gejo, and K. Honma, J. Electron Spectrosc. Relat. Phenom. **184**, 134 (2011).
[14] O. Takahashi, S. Yamanouchi, K. Yamamoto, and K. Tabayashi, Chem. Phys. Lett. **419**, 501 (2006).
[15] K. Tabayashi, M. Chohda, T. Yamanaka, O. Takahashl, and H. Yoshida, Nuc. Instrum. Methods Phys. Res. **A619**, 388 (2010).
[16] Y. Tamenori, K. Okada, O. Takahashi, S. Arakawa, K. Tabayashi, A. Hiraya, T. Gejo, and K. Honma, J. Chem. Phys. **128**, 124321 (2008).

[17]Y. Tamenori, O. Takahashi, K. Yamashita, T. Yamaguchi, K. Okada, K. Tabayashi, T. Gejo, and K. Honma, J. Chem. Phys. **131**, 174311 (2009).
[18]The change in CEBE upon cluster formation is due to the electrostatic interaction between the positive core-hole state of the particular core-atom considered and the surrounding molecules, and possible charge-transfer of the core-atom participated in the H-bonding (D−H···A) system. The term "*intermolecular core-hole interaction*" refers to the former interaction where induced polarization and relaxation effects in the ionization process are also involved.
[19]*Handbook of Chemistry and Physics*, edited by R. C. Weast (CRC, Boca Raton, 2000).
[20]E. H. T. Olthof, A. van der Avoird, and P. E. S. Wormer, J. Chem. Phys. **101**, 8430 (1994); J. S. Lee and S. Y. Park, *ibid.* **112**, 230 (2000); A. D. Boese, A. Chandra, J. N. L. Martin, and D. Marx, *ibid.* **119**, 5965 (2003).
[21]J. A. Altmann, M. G. Govender, and T. A. Ford, Mol. Phys. **103**, 949 (2005).
[22]S. A. Kulkarmi and R. K. Pathak, Chem. Phys. Lett. **336**, 278 (2001); F. M. Abu-Awwad, J. Mol. Struct.: THEOCHEM **683**, 57 (2004).
[23]S. Tada, C. Harada, H. Yoahida, S. Wada, A. Hiraya, K. Tanaka, and K. Tabayashi, J. Chem. Phys. **123**, 124309 (2005).
[24]K. Tabayashi, T. Maruyama, K. Tanaka, H. Namatame, and M. Taniguchi, AIP Conf. Proc. **879**, 1788 (2007).
[25]W. C. Willey and I. H. McLaren, Rev. Sci. Instr. **26**, 1150 (1955).
[26]K. C. Prince, L. Avaldi, M. Coreno, R. Camilloni, and M. de Simone, J. Phys. B **32**, 2551 (1999).
[27]M. J. Frisch, G. W. Trucks, H. B. Schlegel *et al.*, GAUSSIAN 03, Revision C.02, Gaussian, Inc., Wallingford, CT, 2004.
[28]J. B. Foresman and A. Frish, *Exploring Chemistry with Electronic Structure Methods*, 2nd ed. (Gaussian, Inc., Pittsburgh, PA, 1993).
[29]P. Sinha, S. E. Boesch, C. Gu, R. A. Wheeler, and A. K. Wilson, J. Phys. Chem. A **108**, 9213 (2004).
[30]S. F. Boys and F. Bernardi, Mol. Phys. **19**, 533 (1970).
[31]K. Hermann, L. G. M. Pettersson, M. E. Casida, C. Daul, A. Goursot, A. Koester, E. Proynov, A. St-Amant, D. R. Salahub, V. Carravetta, H. Duarte, N. Godbout, J. Guan, C. Jamorski, M. Leboeuf, V. Malkin, O. Malkina, M. Nyberg, L. Pedocchi, F. Sim, L. Triguero, and A. Vela, StoBe-deMon version 2.1, StoBe Software, 2005.
[32]L. Triguero, L. G. M. Pettersson, and H. Ågren, Phys. Rev. B **58**, 8097 (1998).
[33]L. Triguero, O. Plashkevych, L. G. M. Pettersson, and H. Ågren, J. Electron Spectrosc. Relat. Phenom. **104**, 195 (1999).
[34]O. Takahashi and L. G. M. Pettersson, J. Chem. Phys. **121**, 10339 (2004).
[35]W. Kutzelnigg, U. Heischer, and M. Schindler, *NMR-Basic Principles and Progress* (Springer, Heidelberg, 1990).
[36]J. P. Perdew and Y. Wang, Phys. Rev. B **33**, 8800 (1986); **45**, 13244 (1992).
[37]C. Kolczewski, R. Puttener, O. Plashkexych, H. Ågren, V. Staemmler, M. Martins, G. SneII, A. S. Schlachter, M. Sant'Anna, G. Kaindl, and L. G. M. Pettersson, J. Chem. Phys. **115**, 6426 (2001).
[38]R. N. S. Sodhi and C. E. Brion, J. Electron Spectrosc. Relat. Phenom. **36**, 187 (1985).
[39]J. Schirmer, A. B. Trofimov, K. J. Randall, J. Feldhaus, A. M. Bradshaw, Y. Ma, C. T. Chen, and F. Sette, Phys. Rev. A **47**, 1136 (1993); A. Jurgensen and R. G. Cavell, Chem. Phys. **273**, 77 (2001); A. Lindgren, M. Gisselbrecht, F. Burmeister, A. Naves de Brito, A. Kivimaki, and S. L. Sorensen, J. Chem. Phys. **122**, 114306 (2005).
[40]W. L. Jolly, K. D. Bomben, and C. J. Eyermann, At. Data Nucl. Data Tables **31**, 433 (1984).
[41]T. Yamanaka, Master thesis, Hiroshima University, 2009.
[42]O. F. Hagena, Z. Phys. D **4**, 291 (1987); R. Karnbach, M. Joppien, J. Stapelfeld, J. Wörmer, and T. Möller, Rev. Sci. Instrum. **64**, 2838 (1993).
[43]J. G. Loeser, C. A. Schmuttenmaer, R. C. Cohen, M. J. Elrod, D. W. Steyert, R. J. Saykally, R. E. Bumgarner, and G. A. Blake, J. Chem. Phys. **97**, 4727 (1992); E. N. Karyakin, G. T. Fraser, J. G. Loeser, and R. J. Saykally, *ibid.* **110**, 9555 (1997).
[44]A. Halkier, T. Helgaker, P. Jϕrgensen, W. Klopper, H. Koch, J. Olsen, and A. K. Wilson, Chem. Phys. Lett. **286**, 243 (1998); K. A. Peterson, A. K. Wilson, D. E. Woon, and T. H. Dunning, Jr., Thor. Chem. Acc. **97**, 251 (1997).
[45]T. A. Beu and U. Buck, J. Chem. Phys. **114**, 7848 (2001)
[46]A. Bondi, J. Phys. Chem. **68**, 441 (1964).
[47]The positive chemical shift, ΔCEBE > 0 obtained for the pure H-acceptor nitrogen is consistent with the general trend calculated for O−H···O hydrogen-bonded dimers by Ågren's group, see G. Tu, Y. Tu, O. Vahtras, and H. Ågren, Chem. Phys. Lett. **468**, 294 (2009), and references therein.
[48]The interaction that stabilizes a cluster core-ionization state over the corresponding monomer state decreases the core-ionization energy of the cluster relative to the monomer one.
[49]P. Aplincourt, C. Bureau, J.-L. Anthoine, and D. P. Chong, J. Phys. Chem. A **105**, 7364 (2001).